

DRAGANA BOŽIĆ¹
MILAN GORGIEVSKI²
VELIZAR STANKOVIĆ²
MILORAD CAKIĆ³
SILVANA DIMITRIJEVIĆ¹
VESNA CONIĆ¹

¹Mining and Metallurgy Institute
Bor, Bor, Serbia

²University of Belgrade, Technical
Faculty in Bor, Bor, Serbia

³University of Niš, Faculty of
Technology in Leskovac,
Leskovac, Serbia

SCIENTIFIC PAPER

UDC 66.081.3:544.723:546.815

BIOSORPTION OF LEAD IONS FROM AQUEOUS SOLUTIONS BY BEECH SAWDUST AND WHEAT STRAW

Article Highlights

- Beech sawdust and wheat straw can be successfully used for the sorption of lead ions
- During the sorption process the pH changes with time
- Kinetics of metal ions sorption is reasonably fast
- The Temkin isotherm model has shown the best fit with the experimental data
- Maximum sorption capacity for lead ions on the used adsorbents was almost 10 mg g⁻¹

Abstract

This paper presents the results of the Pb²⁺ adsorption from synthetic Pb(NO₃)₂ solutions, using the beech sawdust and wheat straw as adsorbents. Physico-chemical characterization of the adsorbents included the specific surface area, pH_{pzc}, SEM-EDS and FTIR analysis. Adsorption kinetics and isotherms, as well as changes in the pH solution during the process, were monitored and analyzed. The results showed that the adsorption is well explained by the pseudo-second order kinetic model for both adsorbents. Adsorption of the Pb²⁺ on sawdust and straw is well described by the Temkin isotherm, which is confirmed by the high values of the regression coefficient R². The maximum adsorption capacity of lead ions on the beech sawdust and wheat straw was 9.9 and 9.7 mg g⁻¹, respectively. The obtained results have indicated that the beech sawdust and wheat straw are suitable adsorbents for the adsorption of lead ions from dilute aqueous solutions.

Keywords: biosorption, Pb²⁺, beech sawdust, wheat straw, adsorption isotherms.

Discharging the industrial, mining and metallurgical effluents, containing various heavy metal ions into the surface water streams, represents a significant concern for the society and a great threat to the environment due to their toxicity, which could cause severe problems to the organisms living in the waters. As a result of uncontrolled wastewater discharge, the pollution level of the environment has particularly increased during the first half of the 20th century. In order to respond to the pollution of surface and groundwater, the scientists and industry have faced a great challenge to try to improve or even completely replace the industrial processes with new cleaner tech-

nologies that have to reduce or completely eliminate the harmful effects of industrial or mining operations on the environment. This particularly took place during the last three decades of the past century and continues until today [1,2]. There are still the industrial and mining areas affecting the environment, less in developed, but much more in developing countries. The main causes of the water pollution by heavy metals are wastewaters from urban areas; water originating from active or abandoned mines; effluents from ferrous and non-ferrous metallurgy [3,4]; waters from the textile and leather processing industry; from electronics; and, especially, from agricultural activities using various phytochemicals, which partly penetrate into the ground by rain, or otherwise fall and remain there for a long time, affecting ground pollution and the underground waters, or rivers and creeks flowing through the agricultural areas [1,5,6].

Heavy metal ions are as a rule toxic and some of them make organo-metallic cancerous substances,

Correspondence: D. Božić, Mining and Metallurgy Institute Bor, Zeleni bulevar 35, 19210 Bor, Serbia.
E-mail: dragana.bozic@irmbor.co.rs
Paper received: 13 November, 2019
Paper revised: 21 May, 2020
Paper accepted: 16 June, 2020

<https://doi.org/10.2298/CICEQ191113021B>

which enter living organisms through the food chain [2]. In this view, the lead ions and their various compounds are particularly harmful in general for the living world. The increased lead level, for example, accumulated in a human body, can cause severe renal and other impairments, such as: hepatitis, anemia, infertility in women, as well as nerve diseases. According to the physico-chemical properties of lead, Pb^{2+} can easily replace Ca^{2+} in calcified tissues (bones and teeth), but can also form a variety of soluble complexes with bioligands in biological fluids and tissues. Plants can also adsorb and accumulate lead, either from ground or water containing lead compounds, into their roots, stalks, fruits or leaves, depending on the plant species [4,8]. Wastewater from the smelters and foundries of lead, glass and ceramic production, lead battery industry, weapon and ammunition industry contain a substantial amount of lead, approximately around 100 ppm or less [3]. In mine waters the lead concentration is usually less than 1 ppm. Elimination of lead from such wastewater prior to its discharge into the environment is a great challenge for researchers working in various disciplines, due to its extremely harmful effect on organisms.

Various methods for heavy metals removal from industrial effluents can be successfully applied today for this purpose. One of the new approaches that can be efficient in the removal of lead ions from wastewater is adsorption - a technique that can eliminate metal ions to very low concentrations [7]. Biosorption is a new direction within adsorption, in which, instead of classical adsorbents, different living materials are used.

Biosorption

The adsorption process of metal ions can take place on various plant materials, and such a phenomenon is named in the relevant literature as biosorption, while the plant material itself is called biosorbent [9,10]. Biosorption is a process for heavy metal ions removal from the wastewater that has induced a great interest of researchers all over the world. Intensive investigations have been carried out using various combinations of biosorbents and heavy metal ions, for now, at a laboratory scale, in order to form a new technological process, integrating the adsorption of metal ions on biomass with its combustion after loading for the green energy production [11,12]. The basic advantage of biosorption, over other methods of wastewater treatment, is that the biosorbents can efficiently purify those industrial solutions having lower concentration of pollutants, reaching the close output

concentration, or even lower than the MAC is, for a considered ion [10].

Extensive research has shown that many agricultural by-products, as well as the other waste materials from food or wood industries, can be used as biosorbents for the adsorption of heavy metal ions from wastewater [13,40,41]. Materials that were tested as potentially possible low-cost sorbents were: walnut and nut shell, spent grain, olive stones, peanut skins, onion and orange peels, rice husks, leaves, coffee and tea waste, tree fern and other similar plant waste materials [7].

Special attention has been focused on the lingo-cellulose biosorbents, such as bark, leaves, or the wooden mass of various trees. Sawdust, which has exhibited a significant potential as biosorbent, has particularly attracted the attention of researchers working in the wastewater purification area [9,10].

Besides sawdust of various sorts of trees, the straw of different crops has also been proved as a potentially effective biosorbent for the adsorption of metal ions from aqueous solutions [14,10]. Straw and sawdust are mainly composed of cellulose, hemicelluloses, lignin, saccharine and other compounds. Straw contains different functional groups, such as hydroxyl-, carboxyl-, sulfhydryl-, amino- and amide-groups, which can be potentially active sites for attracting and bonding of metal ions [15]. Wheat-, rice-, oats- or barley-straw is particularly convenient to be used in such research due to their widespread presence and easy accessibility, as well as for a massive worldwide production.

The main objective of this work is to designate the adsorption ability of beech sawdust and wheat straw towards lead ions, as well as to determine the effect of various parameters on the adsorption process and to get an insight on the adsorption kinetics and mechanism of lead ions attracting to the used biosorbents. The process equilibrium *via* adsorption isotherms will also be considered. Synthetic solutions of different concentration of lead ions will serve as a model system in this study.

EXPERIMENTAL

Materials

Synthetic salt solutions of $Pb(NO_3)_2$ (MERCK), were used for the adsorption of lead ions. The parent solution with a concentration of 0.2 g dm^{-3} having the initial pH value of 5.65.

Wheat straw was collected from the local fields in the vicinity of Bor (Eastern Serbia), while beech sawdust was taken from a local saw mill. A mono-

sized sieve fraction (-1 + 0.4) mm of both biosorbents was used in the adsorption experiments.

Methods

Characterization of the biosorbents

Specific surface area. The specific surface area of beech sawdust and wheat straw of the chosen sieve fraction (-1 + 0.4) mm, was determined by the adsorption method using a solution of methylene blue, as follows in the reference [16]. UV-Vis spectrophotometer (PU 8620 UV/Vis) was used to determine methylene blue concentration.

Point of zero charge (pH_{pzc}). The point of zero charge (pH_{pzc}) is the pH value of solution, where the surface charge density is equal to zero, *i.e.*, at that point the number of positively charged sites is equal to the number of negatively charged sites [17]

SEM and EDS measurements

Morphology of beech sawdust and wheat straw was analyzed, before and after the adsorption of Pb^{2+} , using a scanning electron microscope (JSM IT 300LV JEOL) with an integrated energy-dispersive X-ray detector (X-max SDD 170 mm², Oxford Instruments). Both samples of biosorbents before scanning were steamed with a thin layer of gold in a sputter coater (JOEL JFC-1300) making them conductive. The prepared samples were then transferred into a microscope chamber and micro photos were taken at voltage of 20 kV. The EDS analysis was done by recording several points on the surface of samples in order to better detect a heterogeneous distribution of elements.

FTIR

Infrared spectra of the investigated samples were recorded using a Bomem MB-100 (Hartmann & Braun, Canada) FTIR spectrometer, in a range of 4000–400 cm⁻¹, at the resolution of 2 cm⁻¹ and with 16 scans. Prior the analysis, the samples were compressed in potassium bromide (KBr) to form tablets. The obtained FTIR spectra were then analyzed using Win Bomem Easy software.

Adsorption of lead ions on the beech sawdust and wheat straw

The adsorption experiments were carried out in laboratory beakers, each equipped with a magnetic stirrer, in order to keep the biosorbent in suspension. Stirring rate was kept constant in all experiments, and was 300 min⁻¹. Prior the adsorption experiments, the biosorbents were washed with 200 cm³ of distilled water and afterwards dried. Two series of adsorption

experiments were carried out to study the adsorption kinetics and adsorption equilibrium.

Synthetic solution of Pb^{2+} , concentration of 0.2 g dm⁻³, was used as an aqueous phase for the kinetic experiments. Mass of 1 g of previously washed and dried biosorbent (beech sawdust or wheat straw) was brought into contact with 50 cm³ of synthetic $Pb(NO_3)_2$ solution for different contact time. After a certain time, the suspension was filtered and the filtrate was analyzed on the Pb^{2+} content. In parallel with this, the concentration of alkali and alkaline earth metal ions was determined with the aim of trying to describe the mechanism of the adsorption process, as well as to determine the cation exchange capacity.

Concentrations of lead ions, as well as alkali and alkaline earth metal ions, were determined using the atomic absorption spectrophotometer (Perkin-Elmer 403 AAS).

The adsorption capacity of biosorbent q_t is defined as a mass of ions adsorbed on the unit mass of biosorbent, at constant temperature [18,19]. The adsorption capacity, as well as its change with the adsorption time, was determined from the mass balance, according to the following equation:

$$q_t = \frac{c_i - c_t}{m} V \quad (1)$$

where: q_t is the mass of adsorbed metal per unit mass of adsorbent (mg g⁻¹) at time t ; c_i and c_t are the initial and actual concentrations of metal ions at time t (mg dm⁻³); V - volume of treated solution (dm³); m - mass of adsorbent (g). The adsorption degree (AD) is defined as the percentage of adsorbed metal ions, described by the following relationship:

$$AD = 100(1 - c_t / c_i) \quad (2)$$

It represents an ability of how many metal ions can be removed from a solution by a particular biosorbent. AD is also an indicator of the adsorbent saturation, as well as the solution depletion, *i.e.*, of the process completion.

During the adsorption, a change of the solution pH value was also monitored with time. All experiments were carried out at the ambient temperature.

A series of experiments was carried out contacting a constant mass of adsorbent (1 g) with the equal volume of solution (0.05 dm³), which contained different initial concentrations of metal ions in a range from 0.005 to 0.2 g dm⁻³. The phases were kept in suspension with a magnetic stirrer for a period of 60 min, considering that this contact is long enough to achieve equilibrium between phases [7,20]. After-

wards, the suspension was filtered, and filtrate analyzed for the residual content of lead ions.

Pseudo-first- and pseudo-second order reaction kinetic models

For modeling the adsorption process rate, two kinetic models were tested, *i.e.*, the pseudo-first- and pseudo-second order kinetic model, and compared with the experimental data. The pseudo-first order kinetic model can be expressed by the following differential equation [31]:

$$\frac{dq_t}{dt} = k_1(q_e - q_t) \quad (3)$$

or, in its integral form, as a linear equation in a system with semi-logarithmic coordinates:

$$\log(q_e - q_t) = \log q_e - \frac{k_1}{2.303} t \quad (4)$$

where: q_e - is the adsorption capacity at equilibrium (mg g^{-1}); q_t - is the adsorption capacity at the process time t (mg g^{-1}); k_1 - is the constant rate of the pseudo-first reaction order (min^{-1}); and t - is the process time (min).

The differential equation, describing the pseudo-second reaction order kinetics may be presented as:

$$\frac{dq_t}{dt} = k_2(q_e - q_t)^2 \quad (5)$$

The integral form of Eq. (5) will be:

$$\frac{1}{(q_e - q_t)} = \frac{1}{q_e} + k_2 t \quad (6)$$

Rearranging Eq. (6) to get it in a linear form, leads to the following equation:

$$\frac{t}{q_t} = \frac{1}{k_2 q_e^2} + \frac{t}{q_e} \quad (7)$$

where k_2 is the adsorption rate constant for the pseudo-second reaction order ($\text{g mg}^{-1} \text{min}^{-1}$).

RESULTS AND DISCUSSION

Physical, chemical and physicochemical characteristics of the biosorbents

The beech sawdust moisture was 8.5%, while the wheat straw was 7.23%, both calculated on the

initial biosorbent weight. It can be said that there is no significant moisture difference between the used biosorbents due to their similar way of storage, *i.e.*, both were packed in paper bags and stored in a laboratory chamber under the same humidity.

The fraction of sawdust ash was 2.06%, based on the initial weight of dried sawdust, while the ash fraction from straw was almost three times higher and amounted to 6.2%, calculated on dry straw. Chemical composition of both ashes is shown in Table 1.

Obviously, with the exception of MgO, SiO₂ and MnO content, which are almost equal in both ashes, there is a strong difference in the chemical composition between ashes of these two biosorbents. It can be seen, from Table 1, that the beech sawdust ash has a dominant CaO content, which is approximately three times higher than the one in the wheat straw ash. Unlike the beech sawdust, the wheat straw contained much more alkali metals than the beech sawdust. So, the K₂O content in the wheat straw ash was more than 6 times higher than in the sawdust ash, while Na₂O was about 2.5-3 times higher. Special attention was paid here to the content of alkali and alkaline earth metals in the straw and sawdust, due to their impact, particularly calcium and potassium, on the adsorption process, which will be considered through further text. Physical and physicochemical properties of the considered biosorbents are summarized and presented in Table 2.

Table 2. Physical and physicochemical properties of the biosorbents

Biosorbent property	Beech sawdust	Wheat straw
Specific surface area, $\text{m}^2 \text{g}^{-1}$	1.08 [3,7,17]	1.54 [3,7,17]
Moisture, %	8.5	7.23
COD, $\text{mg O}_2 \text{dm}^{-3}$	0.8	18
CEC/ $\text{mmol Me}^{z+} \text{g}^{-1}$	1.45	1.86
Point of the zero charge, pH_{pzc}	7.4 [3,7,17]	6.7 [3,7,17]

The content of organic substances in water from straw washing, expressed as a chemical oxygen demand (COD), is about 22.5 times higher than the content of organic substances in water from sawdust washing [17]. It means that the content of soluble organic substances, which could be transferred from the biosorbents into the aqueous phase, is much higher in the case of wheat straw than in the case of

Table 1. Chemical composition (mass%) of beech sawdust and wheat straw ash

Material	Na ₂ O	K ₂ O	MgO	CaO	Fe ₂ O ₃	SiO ₂	SO ₃	Al ₂ O ₃	P ₂ O ₅	TiO ₂	MnO	Others
Sawdust	1.51	4.56	3.32	22.39	3.00	34.08	24.7	4.73	1.17	0.18	0.13	0.17
Straw	4.14	28.62	3.25	6.83	0.55	36.36	16.12	0.29	3.0	0.017	0.11	0.173

beech sawdust. This issue must be taken into consideration, in particular how to treat water from washing the wheat straw before its discharging, or to use it as a fertilizer for watering a plantation, for example.

Based on the results shown in Table 2, the total cation exchange capacity (*CEC*), expressed as a sum of alkali and alkaline earth ions, transferred from the solid to the aqueous phase, is slightly higher for the wheat straw.

As shown in Table 2, the corresponding pH_{pzc} values for the wheat straw and beech sawdust are close to each other, and were 6.7 and 7.4, respectively. It means that at $pH < 6.7$ for wheat straw, or < 7.4 for beech sawdust, the surface area of the corresponding adsorbent is positively charged, while at $pH > 6.7$ for straw, or > 7.4 for sawdust, the surface area of the adsorbent will be negatively charged.

Rinsing of the biosorbents

Rinsing of both sawdust and straw was carried out from two reasons:

- in order to remove physically entrained organic and inorganic dirtiness, as fine particles of the biosorbents and earth;
- in order to get an insight on the amount of alkali and alkaline earth metals that will be leached out from the biosorbents at rinsing, as well as to see whether and how the rinsing itself affects the adsorption capacity of the used biosorbents;

The procedure of the rinsing experiments was described in detail elsewhere [12]. After each portion of distilled water passing through a filter, the filtrate was sampled and analyzed on the content of Na^+ , K^+ , Ca^{2+} and Mg^{2+} . Prior the analysis, the pH and conductivity values of filtrate were both measured as well.

Adsorption

Change of alkali and alkaline earth metals concentration at rinsing the biosorbents and after the completion adsorption of Pb^{2+}

Contact between a biosorbent and water solution containing adsorbate, has a twofold effect. Alkali and alkaline earth metals from biosorbents will partly be leached out by water, while a portion of them (mainly calcium and magnesium) will take part in the

ion exchange process with heavy metal ions present in the solution [10]. To get evidence on the amount of these metals, which will be rinsed from biosorbents and how much will be replaced by heavy metal ions from water solution, a series of experiments was carried out, as described earlier.

Table 3 presents the concentrations of alkali and alkaline earth metal ions in filtrate, measured after rinsing the biosorbents with water and after the adsorption of Pb^{2+} .

After rinsing the sawdust and wheat straw (Table 3), the potassium ions have been leached for the most part of the molecular structure of adsorbents. Also, it can be seen that after the adsorption of Pb^{2+} on the sawdust and straw, the Ca^{2+} have been leached for the most part where it is assumed that these ions are largely involved in the process of ion exchange.

Change of the solution pH value with time, during the adsorption of Pb^{2+}

It was remarked in our earlier works [7,9,17] that the pH of solution changes sharply with the adsorption time, particularly in the first few minutes of the process, indicating an interaction between the solid and aqueous phase. In some cases, this change was significant, as it was during the adsorption of Pb^{2+} on the sawdust and straw, which is illustrated in Figure 1.

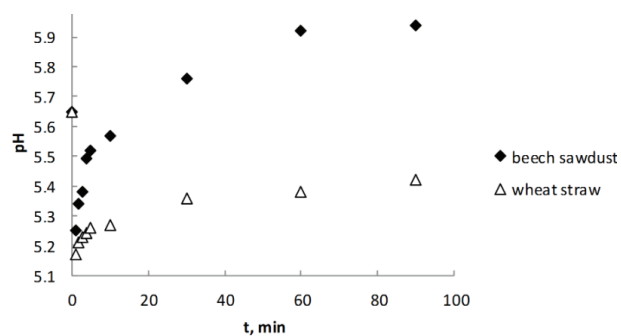


Figure 1. Change of the pH value with time at the adsorption of Pb^{2+} on beech sawdust and wheat straw.

Monitoring the pH value change, in the first few minutes of adsorption (see Figure 1), a sudden drop was observed in the pH at very beginning of the

Table 3. Concentration of alkali and alkaline earth metal ions in the filtrate ($mmol\ g^{-1}$), measured upon the rinsing with distilled water and after adsorption of Pb^{2+}

Procedure	Na^+	K^+	Ca^{2+}	Mg^{2+}
Rinsing of sawdust with distilled water	0.0056	0.0177	0.011	0.003
Rinsing of wheat straw with distilled water	0.0026	0.061	0.011	0.005
Adsorption of Pb^{2+} onto sawdust	0.0018	0.0017	0.00625	0.002
Adsorption of Pb^{2+} onto wheat straw	0.002	0.0058	0.0073	0.005

process, and then an increase during the rest of process, reaching approximately the constant pH value at the end of the experiment. Here, a significant difference in pH behavior was found between the biosorbents. Wheat straw could not achieve the starting pH value of 5.65, approaching steadily to a value of 5.45, while, in case of the sawdust, the pH value reached the initial value within the first 20 min, tending to reach even $\text{pH} \approx 6$ at the end of the process. All these pH changes were taking place during the first 60 min from the start of the process. A dramatic drop, followed with a sudden increase in the pH change, corresponds to the first 20 min of the adsorption process, when the fastest adsorption rate takes place, which is presented in Figure 1. It was assumed that a sudden decrease in the pH value, during the initial stage of the process, is a consequence of a rapid replacement between the Pb^{2+} and hydrogen atoms from the functional groups contained in a molecular structure of biosorbents. Further adsorption is carried out by a substitution of calcium atoms from biosorbent structure with Pb^{2+} and, in parallel with the ion exchange reactions between the Pb^{2+} and H^+ from hydroxylic and phenolic functional groups from the cellulose structure [17], leading to a further increase in the pH of the aqueous phase for almost 0.7 in the case of sawdust, while in the case of wheat straw, a smaller increment of the pH appeared of approximately 0.3.

SEM-EDS analysis of beech sawdust and wheat straw

Based on the SEM analysis, the structure of the adsorbents' surface was visually examined. A certain difference in the structure between the untreated beech sawdust and wheat straw were observed, and the corresponding ones after the adsorption of lead ions. The SEM images of the surface morphology of the beech sawdust and wheat straw, before and after the adsorption of lead ions are shown in Figure 2a-d.

Figure 2a and c presents the micrographs of the surface of untreated beech sawdust and wheat straw. The macro-pores and cavities of larger dimensions inside the particles can be seen. The presence of macro-pores and cavities facilitates an easier movement of the aqueous phase through the structure of adsorbents, causing an easy transfer of metal ions through the internal particles structure and reaching the active sites at the internal surface to be adsorbed on [21,22].

After the adsorption of lead ions onto beech sawdust and wheat straw, the SEM images have also been taken - Figure 2b and d, in which a modified surface morphology of the adsorbents, compared to the untreated one, can be observed. A relatively compact and uniformly ordered lamellar structure of the particles is observed after the adsorption of lead ions

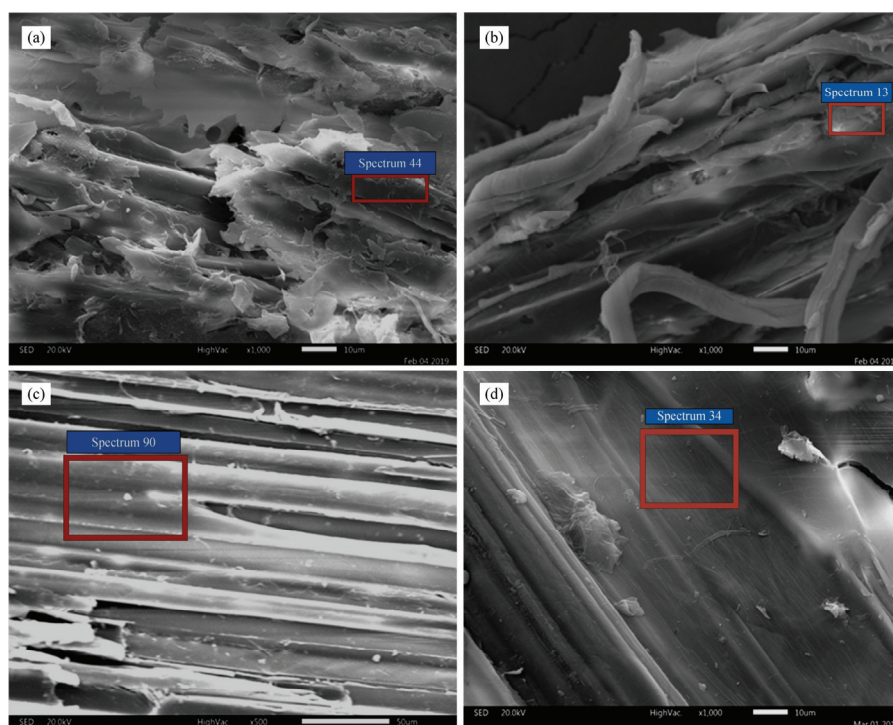


Figure 2. SEM images of beech sawdust and wheat straw: a) beech sawdust after rinsing with distilled water (1000x magnification); b) beech sawdust after adsorption of lead ions (1000x magnification); c) wheat straw after rinsing with distilled water (500x magnification); d) wheat straw after adsorption of lead ions (1000x magnification).

on them. In relation to the morphology of untreated adsorbents, Figure 2a and c, a change in the morphology is evident in Figure 2b and d, which is manifested by a compact cellulose structure, as a result of incorporation of the lead ions into the molecular structure. These changes in the morphology suggest that the biosorption of lead ions is associated with the chemical changes in the surface of adsorbents, what was confirmed by the FTIR analysis and will be discussed through the next subtitle.

The EDS analysis of beech sawdust and wheat straw was done by selection several points on the surface of samples to detect a heterogeneous distribution of elements. The peaks for C, O and Ca can be observed in Figure 3a, spectrum 44, for the untreated beech sawdust. After adsorption of lead ions (Figure 3b, spectrum 13), the peaks for Ca disappeared while the peaks for Pb occur. This indicates that calcium was replaced by lead in the ion exchange process.

The peaks for C, O, Si, Ca, K and Mg can be observed on the EDS spectrum of untreated wheat straw, (Figure 3c, spectrum 90). After adsorption of lead ions (Figure 3d, spectrum 34), the peaks for Si, Ca, K and Mg disappeared, while several peaks for Pb occurred, which clearly indicates that besides Ca, K and Mg also take part in the ion exchange process with lead ions.

FTIR analysis of beech sawdust and wheat straw

The lignocelluloses materials have a complex chemical composition. Therefore, the FTIR spectro-

scopy is mainly used to compare the FTIR spectra of biosorbents before and after the adsorption process, in order to identify the functional groups responsible for the adsorption of metal ions. The adsorption bands in the range from 1300 to 1000 cm^{-1} correspond to $-\text{OH}$, $\text{C}-\text{OH}$, and $-\text{O}-\text{C}-\text{O}$ vibrations of the glycoside cellulose groups. The adsorption bands corresponding to a deformation of $\text{CH}-$ groups appear in the range from 1000 to 700 cm^{-1} [23–26].

Bands from 1730 to 1260 cm^{-1} originate from the $-\text{C}-\text{OH}$, $\text{CH}-$, $-\text{CH}_2$ and $\text{C}=\text{O}$ vibrations, and are typical for hemicelluloses. Bands from 1600 to 1260 cm^{-1} correspond to the $\text{C}=\text{C}$ and $-\text{OCH}_3$ vibrations, typical for lignin. At the low-frequency area of the spectra, from 600 to 400 cm^{-1} , the bands from valent $-\text{O}-\text{M}$ vibrations are expected, indicating a metal interaction with biosorbent. At the high frequency area of the spectra, around 3400 cm^{-1} , bands of the valent $-\text{OH}$ (alcohols and phenols), as well as the $=\text{NH}$ vibrations are expected [27]. Figures 4 and 5 present a set of the FTIR spectra of rinsed adsorbents and those after the adsorption of Pb^{2+} .

An adsorption band around 1735 cm^{-1} can be observed on both spectra. It corresponds to a $\text{C}=\text{O}$ group of aldehydes and ketones, the position of which is shifted to the lower frequencies, and whose intensity is decreased significantly after the adsorption process, indicating that this functional group is involved in the capturing of lead ions. Bands in the area under 600 cm^{-1} (marked by the arrows on both

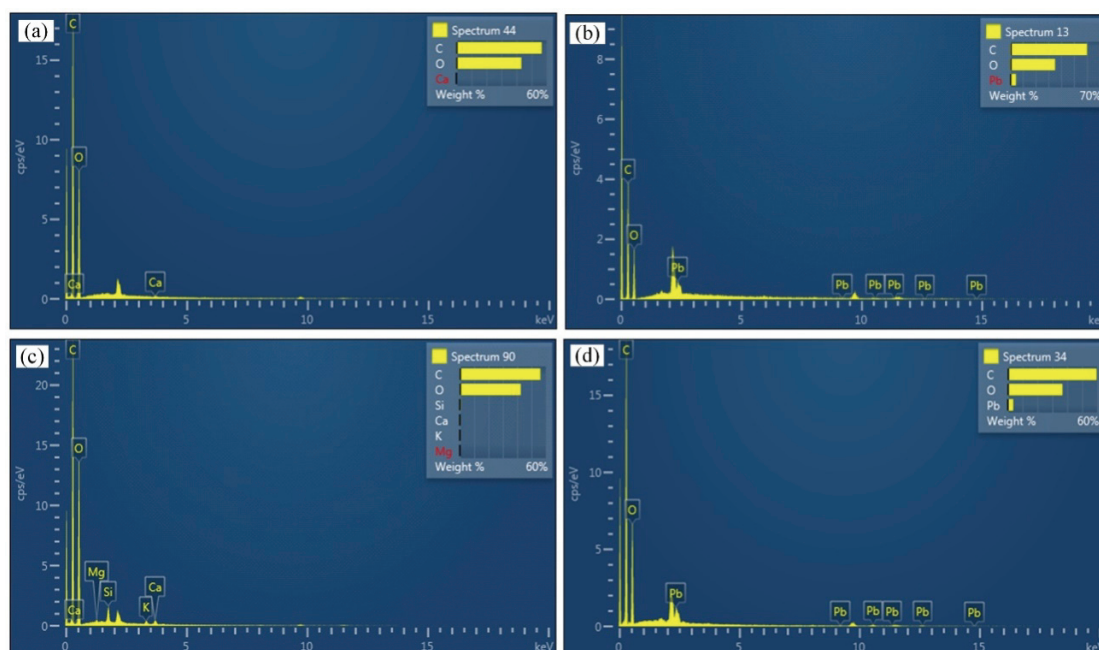


Figure 3. EDS spectra of beech sawdust and wheat straw: a) raw beech sawdust; b) beech sawdust after adsorption of lead ions; c) raw wheat straw; d) wheat straw after adsorption of lead ions.

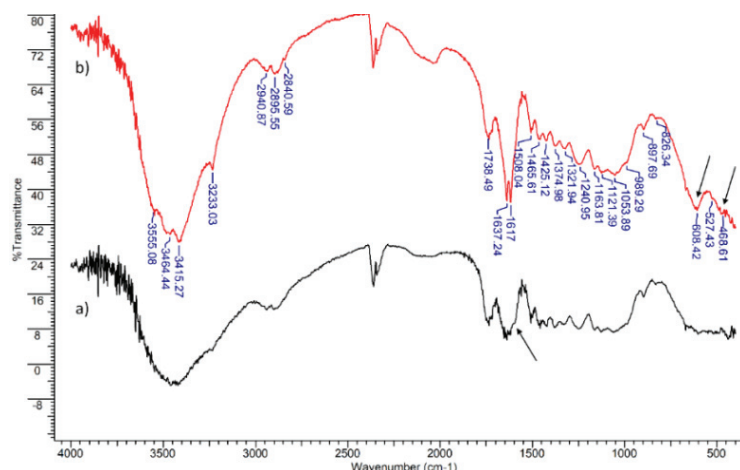


Figure 4. FTIR spectra of beech sawdust: a) after rinsing with distilled water; b) after adsorption of Pb^{2+} .

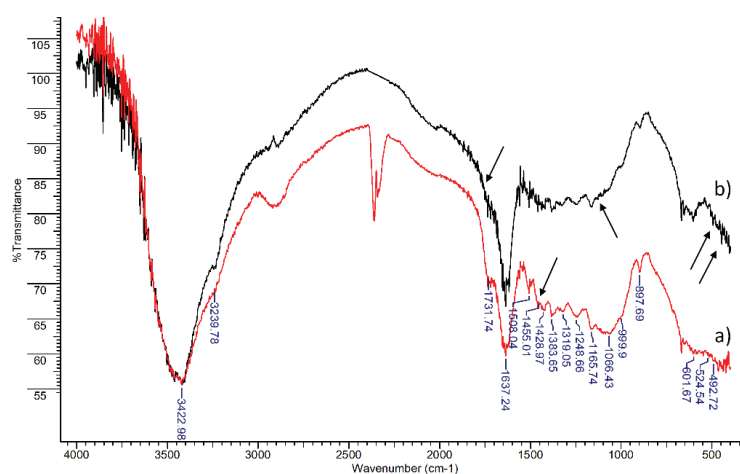


Figure 5. FTIR spectra of wheat straw: a) after rinsing with distilled water; b) after adsorption of Pb^{2+} .

spectra) correspond to the valent O–Pb vibrations. It was observed that the number of bands decreases for beech sawdust in a domain of valent vibrations of the unsaturated groups of aromatic type (1650 cm^{-1}), while the frequency gets slightly lower after the adsorption of Pb^{2+} . Changes in the valent –OH groups are observed, indicating that in addition to the C=O group, the –OH and aromatic groups are also responsible for the adsorption of Pb^{2+} [28].

Rate of the Pb^{2+} adsorption

Kinetics of the Pb^{2+} adsorption was investigated with the aim of obtaining an insight in the overall adsorption rate and adsorption reaction order, as well as to derive the reaction rate constants for the used biosorbents, also, to get data on the amount of adsorbed metal ion exchange with time, as well as the process time required to achieve the adsorption equilibrium between the aqueous and solid phase for given experimental conditions. The process time was kept constant and was 90 min in all experiments. The

process time is an important parameter affecting the adsorption process rate [29], which changes gradually in such a way that the rate is high at the process beginning and then decreases, approaching almost a zero value at equilibrium. Here, the adsorption capacity change with time is presented in Figure 6.

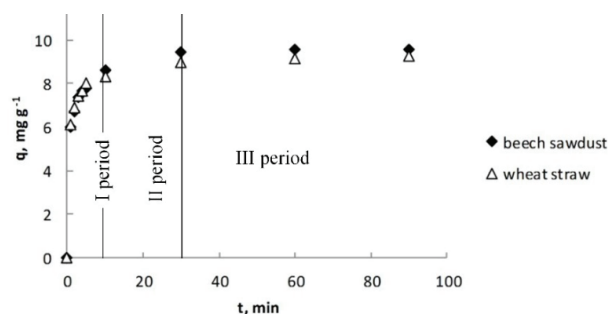


Figure 6. Change in the adsorption capacity of the Pb^{2+} with time: on beech sawdust and wheat straw.

Looking at the curves shape, three periods of the process rate are easily recognizable. In the I

period, the adsorption capacity of Pb^{2+} rises rapidly up within the first 10-15 min, meaning a fast occupation of free sites on the easily accessible surface by the Pb^{2+} and their adsorption on them. After the fast I period, the process entered in the II period, when Pb^{2+} must penetrate into the internal structure of biosorbent particles to find vacant active sites to be adsorbed on. It is assumed that, during the II period, with a slower adsorption rate, the adsorption is limited by a diffusion transport of Pb^{2+} through the adsorbent internal structure, consisting from the macro- and micro-pores and counter-current flux of the exchanged ions outwards [7,30]. The rate of q rises more slowly with time, approaching an equilibrium value, which was achieved after 30 min of the process, when an increment in the adsorption capacity against time became almost negligible (III period of the process). In the III period of the adsorption, one may consider that almost all active sites were occupied by the Pb^{2+} , and the process equilibrium is achieved at given experimental conditions. During study of the adsorption kinetics, the maximum achieved adsorption capacity of Pb^{2+} on beech sawdust was 9.6 mg g^{-1} , while it was 9.3 mg g^{-1} for wheat straw. It could be assumed that the adsorption capacities are rather modest than high, and are close to those values obtained for the same or similar biosorbents [9]. The important fact is that the achieved adsorption capacities are almost equal within an interval of $\pm 3\%$. An engineering significance is that both biosorbents could be used with the same efficiency, either in mixture or replacing one with another. By then, the achieved AD , for wheat straw was 96.4%, while for sawdust it has reached almost 99.5%. Both values are encouraging in consideration of the biosorbents use for their potential implementation at the industrial scale. Knowing either maximum achieved adsorption capacity q , or AD at a given process time, a compromise has to be made between these properties and the process time, allowing us to determine a residence time in the adsorber, operating in a batch mode.

Testing of the kinetic models

From Eq. (4), it is possible to evaluate the values of k_1 from the corresponding graph slopes, while q_e can be calculated from the corresponding intercepts of the graphs $\log(q_e - q_t)$ vs. t , as it is

presented in Figure 7, in which the linearized form of the experimental results from Figure 6 are plotted.

The obtained experimental values of q_e and those calculated using Eq. (4), as well as the obtained values of the correlation coefficient (R^2), are summarized and presented in Table 4. It can be seen that the pseudo-first order kinetic model does not describe fairly well the adsorption process. Significant discrepancy, particularly between the computed and experimental q_e values, as well as not so high R^2 values, eliminates the pseudo-first reaction order model from further consideration.

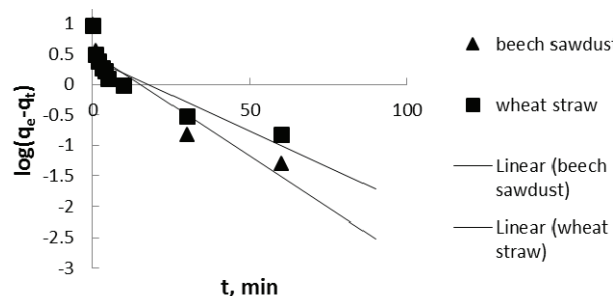


Figure 7. Pseudo-first reaction order model for the lead ions adsorption: on beech sawdust and wheat straw.

A non-linear shape of the curves presented in Figure 6, strongly indicates the biosorption process nature, which follows the pseudo-second reaction order kinetic model, which was pointed out through our earlier works and confirmed by other scientists, working on the metal ions biosorption on various biosorbents [9,10].

A linearized form, given by Eq. (7), is presented in Figure 8, expressed as t/q_t against the process time t . Obviously, a linear dependence is obtained in

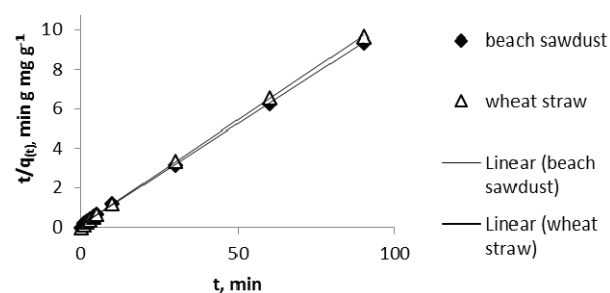


Figure 8. Linearized form of the pseudo-second order reaction for the Pb^{2+} adsorption: on beech sawdust and wheat straw.

Table 4. Kinetic parameters of the Pb^{2+} adsorption on beech sawdust and wheat straw

Adsorbent	Pseudo-first-order kinetic model				Pseudo-second-order kinetic model			
	k_1 / min^{-1}	$q_{e,exp} / \text{mg g}^{-1}$	$q_{e,cal} / \text{mg g}^{-1}$	R^2	$k_2 / \text{g mg}^{-1} \text{min}^{-1}$	$q_{e,exp} / \text{mg g}^{-1}$	$q_{e,cal} / \text{mg g}^{-1}$	R^2
Beech sawdust	0.076	9.6	3.258	0.892	0.125	9.6	12.82	0.999
Wheat straw	0.053	9.3	2.63	0.781	0.152	9.3	11.90	0.999

both considered cases and the experimental data fits well with Eq. (7). Based on the linear dependence, the reciprocal values of q_e were evaluated from the corresponding slopes, while the rate constants k_2 were calculated from the corresponding intercepts for both biosorbents. The obtained experimental values for q_e and those calculated from Eq. (5), as well as the corresponding rate constants and correlation coefficients (R^2) are summarized in Table 4.

Kinetic parameters, obtained using the linear regression analysis for the tested models, as well as the corresponding correlation coefficients R^2 , have shown better fitting with the pseudo-second reaction order kinetic model than with the pseudo-first one for both considered biosorbents. Namely, the adsorption capacity values, calculated using Eq. (4), significantly differ from those experimentally obtained. Experimental values of the adsorption capacity showed a good agreement with those ones calculated using Eq. (6). The obtained correlation coefficients R^2 are also very high in case of the pseudo-second order reaction model in comparison with the pseudo-first one. It means that the adsorption kinetics can be fairly modeled with the pseudo-second reaction order model. The same findings were already reported by us, as well as by other scientists, for some other metal ions and other biosorbents [7,17].

Adsorption isotherms

An adsorption isotherm is a relationship between the concentrations of adsorbed species on the adsorbent surface, q_e , in contact with the same species in the aqueous phase, C_e , at equilibrium at given temperature. Three frequently used relationships of adsorption isotherms are the Langmuir, Freundlich and Temkin isotherm model [15], which were tested with the experimental results obtained in this study in a way described in the experimental part. Experimental data for q_e plotted against the corresponding C_e , for beech sawdust and wheat straw are presented in Figure 9.

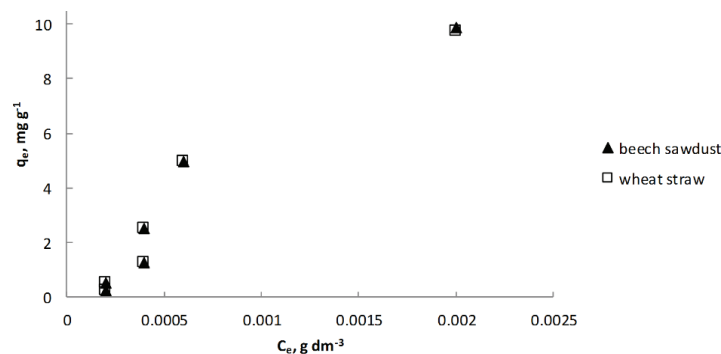


Figure 9. Adsorption isotherms for beech sawdust and wheat straw.

Each of the mentioned isotherm model will be tested with the experimental data in order to determine how they fit to each other.

Langmuir isotherm

This model of isotherm could be described by Eq. (8) [32]:

$$q_e = \frac{q_m K_L C_e}{1 + K_L C_e} \quad (8)$$

where: C_e - equilibrium concentration of metal ions (mg dm⁻³); q_e - mass of adsorbed Pb²⁺ per unit of the biosorbent mass at equilibrium (mg g⁻¹); q_m - maximum adsorption capacity (mg g⁻¹); K_L - the Langmuir constant (dm³ mg⁻¹).

Linearization of Eq. (8) leads to the following relationship:

$$\frac{C_e}{q_e} = \frac{1}{K_L q_m} + \frac{1}{q_m} C_e \quad (9)$$

Figure 10 presents the linearized form of the Langmuir isotherm given by Eq. (9) for beech sawdust (Figure 10a) and wheat straw (Figure 10b) and compared with the experimental data derived from Figure 9. The ratio of C_e/q_e as a function of C_e is a straight line with a slope of $1/q_m$, while the intercept is $1/q_m K_L$. The parameters q_m , K_L and regression coefficient R^2 are summarized in Table 5.

Evidently, there is a significant discrepancy between the experimental data and theoretical lines, so that the Langmuir model cannot be applied for describing the adsorption equilibrium of the considered systems.

Freundlich isotherm

The Freundlich isotherm is used as an empirical model describing the adsorption from the solution over the surface heterogeneity and exponential distribution the active sorbent sites of the sorption material [33]. The Freundlich isotherm is expressed

Table 5. Equilibrium parameters of the adsorption isotherm

Adsorbent	Model									
	Langmuir				Freundlich			Temkin		
	$K_L / \text{dm}^3 \text{mg}^{-1}$	$q_m / \text{mg g}^{-1}$	$q_{exp} / \text{mg g}^{-1}$	R^2	$K_F / \text{dm}^3 \text{g}^{-1}$	n	R^2	K_T	$B / \text{dm}^3 \text{m}^{-1}$	R^2
Sawdust	0.66	16.95	9.9	0.84	190546	0.66	0.847	24.9	2.832	0.97
Wheat straw	128.35	25.97	9.7	0.82	1600	1.12	0.689	24.47	2.77	0.97

by the following equation [2]:

$$q_e = K_F C_e^n \quad (10)$$

Linearization of the relationship (10), leads to the following expression:

$$\log q_e = \log K_F + \frac{1}{n} \log C_e \quad (11)$$

where: K_F - Freundlich constant related to the adsorption capacity ($\text{dm}^3 \text{g}^{-1}$); n - adsorption intensity.

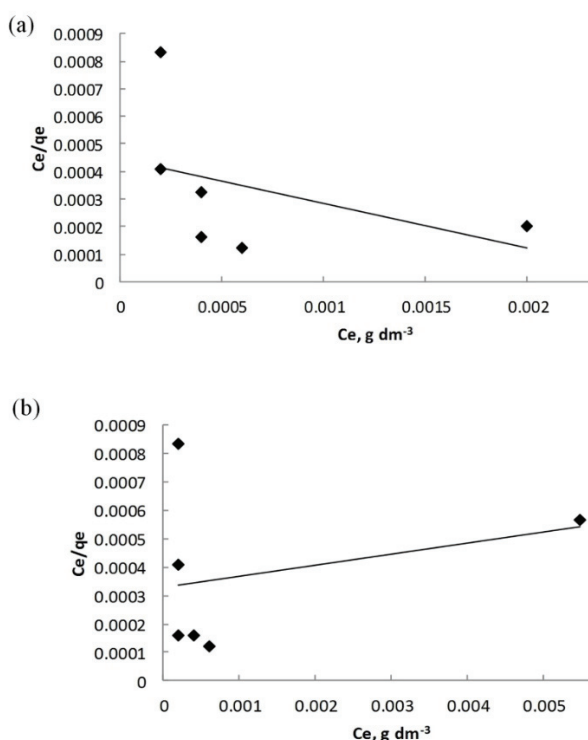


Figure 10. Linearized form of the Langmuir isotherm for beech sawdust (a) and wheat straw (b).

Figure 11 presents the linearized form of the Freundlich isotherm in the log-log coordinate system, together with the corresponding experimental data for sawdust (Figure 11a) and straw (Figure 11b). $\log q_e$ vs. a function of $\log C_e$ should give a straight line with a slope of $1/n$ and intercept $\log K_F$. Parameter $1/n$ relates to the adsorption intensity and varies with material heterogeneity [32]. Parameters n , K_F and R^2 are

also given in Table 5, together with the ones evaluated for the Langmuir adsorption isotherm model.

Here, there is a certain matching between the theory and experimental data for both biosorbents.

Temkin isotherm

The Temkin adsorption isotherm model assumes a uniform distribution of the binding energy to a maximum energy, wherein the interaction between adsorbent-adsorbate, the heat of adsorption of all adsorbates decreases linearly with a degree of surface coverage [8]. The Temkin model is developed to be valid on the whole external and internal surface, including pore walls [34].

The Temkin isotherm is given by the following expression:

$$q_e = B \ln(K_T C_e) \quad (12)$$

It can be developed to the linear form giving the following relationship:

$$q_e = B \ln K_T + B \ln C_e \quad (13)$$

where: B - constant, relating to the adsorption heat ($B = RT/b$) ($\text{dm}^3 \text{m}^{-1}$); b - variable adsorption energy, J mol^{-1} ; K_T - the Temkin isotherm constant ($\text{dm}^3 \text{mg}^{-1}$).

Figure 12 presents the Temkin isotherm in a semi-logarithmic coordinate system, according to Eq. (12), for beech sawdust (Figure 12a) and wheat straw (Figure 12b). Linear dependence of q_e and $\ln C_e$ allows determining values of the constant B , from the corresponding slopes, as well as values of the constant K_T from the corresponding intercepts. Constant K_T corresponds to the maximum energy of binding, while constant B relates to the heat of adsorption. The Temkin isotherm constants B and K_T , as well as the correlation coefficients (R^2), are also given in Table 5.

The adsorption equilibrium of Pb^{2+} on biosorbents is well represented by the Temkin adsorption isotherm model in relation to the Langmuir and Freundlich model, having the highest value of R^2 for both biosorbents (0.971 for beech sawdust and 0.969 for wheat straw), as shown in Figure 12 and Table 5. Similar results were published by other researchers, using the same kind of biosorbents and ions [35–39].

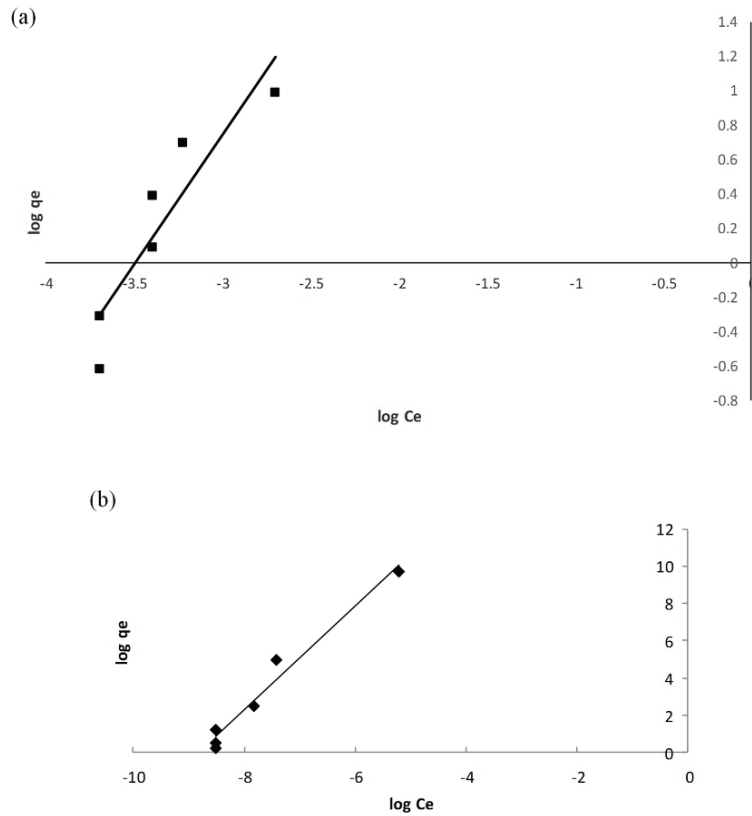


Figure 11. Linearized form of the Freundlich isotherms for beech sawdust (a) and wheat straw (b).

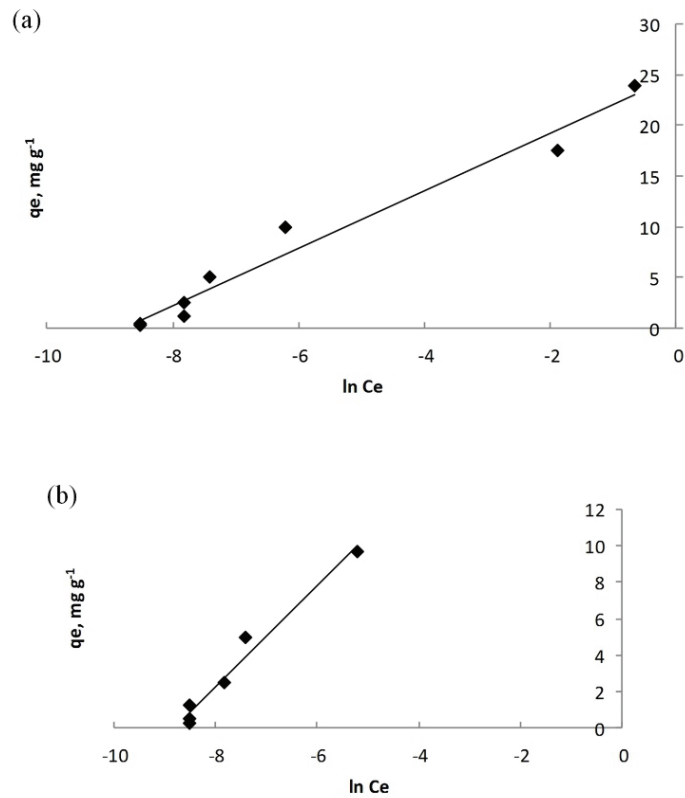


Figure 12. Linearized form of the Temkin isotherms for beech sawdust (a) and wheat straw (b).

CONCLUSION

Based on the analysis of the obtained results, the following conclusions can be derived.

On the SEM micrographs of beech sawdust and wheat straw macro-pores and cavities of larger dimensions can be seen. It is assumed that the lead ions easily penetrate through these pores and cavities into the adsorbents' structure to be adsorbed at the internal active sites. The EDS analysis of used adsorbents was done by recording several points on the surface of samples to detect a heterogeneous distribution of elements. For beech sawdust, calcium could be exchanged with lead during the adsorption process, while for wheat straw Ca, K and Mg were exchanged with lead during the adsorption process.

Based on the FTIR analysis, the C=O group of aldehydes and ketones, –OH and aromatic groups may be responsible for the adsorption of Pb²⁺.

The adsorption kinetics is well described by the pseudo-second-order kinetic model, whereby the chemisorption is a possible way of adsorbate bonding on the surface of the biosorbents.

The Temkin isotherm model has shown the best fit with the experimental data. Maximum achieved adsorption capacity for the adsorption of lead ions was 9.9 mg g⁻¹ for beech sawdust, while it was 9.7 mg g⁻¹ for wheat straw.

Acknowledgements

This work was financially supported by the Ministry of Education, Science and Technological Development of the Republic of Serbia, Grant No. 451-03-9/2021-14/ 200052 and the scientific research work at the University of Belgrade, Technical Faculty in Bor, according to the contract with registration number 451-03-9/2021-14/ 200131.

REFERENCES

- [1] S.S. Ahluwalia, D. Goyal, *Bioresour. Technol.* 98 (2007) 2243-2257
- [2] M. Yurtsever, A. Şengil, *J. Hazard. Mater.* 163(2009) 58-64
- [3] M.N.M. Ibrahim, W.S.W. Ngah, M.S. Norliyana, W.R.W. Daud, M. Rafatullah, O. Sulaiman, R. Hashim, *J. Hazard. Mater.* 182 (2010)377-385
- [4] N.H. Bhatti, S. Ghufrana, A.H.E. Muhammad, *J. Chin. Chem. Soc.* 55 (2008) 1235-1242
- [5] O.S. Lawal, A.R.S. Ajayi, O.O. Rabiun, *J. Hazard. Mater.* 177 (2010) 829-835
- [6] A. Sönmezay, M. Salim, N. Bektaş, *Trans. Nonferrous Met. Soc. China* 22 (2012)3131-3139
- [7] D. Božić, V. Stanković, M. Gorgievski, G. Bogdanović, R. Kovačević, *J. Hazard. Mater.* 171 (2009) 684-692
- [8] S.P. Kumar, C. Vincent, K. Kirthika, K.S. Kumar, *Braz. J. Chem. Eng.* 27 (2010)339-346
- [9] D. Božić, M. Gorgievski, V. Stanković, N. Štrbac, S. Šerbula, N. Petrović, *Ecol. Eng.* 58 (2013) 202-206
- [10] M. Gorgievski, D. Božić, V. Stanković, V. Trujić, *Proceedings of the Faculty of Technology in Leskovac*, 20 (2011) 35-43 (In Serbian)
- [11] V. Stanković, D. Božić, M. Gorgievski, G. Bogdanović, *Chem. Ind. Chem. Eng. Q.* 15 (2009) 237–249
- [12] V. Stanković, M. Gorgievski, D. Božić, *Biomass Bioenergy* 88 (2016) 17-23
- [13] M. Petrović, T. Šoštarčić, M. Stevanović, J. Petrović, M. Mihajlović, A. Čosović, S. Stanković, *Ecol. Eng.* 99 (2017) 83-90
- [14] R. Zhang, J. Zhang, X. Zhang, C. Dou, R. Han, *J. Taiwan Inst. Chem. Eng.* 45 (2014) 2578-2583
- [15] U. Farooq, J.A. Kozinski, M.A. Khan, M. Athar., *Biotechnol. J.* 101 (2010) 5043-5053
- [16] M.R. Unnitham, T.S. Anirudham, *Ind. Eng. Chem. Res.* 40 (2001) 2693-2701
- [17] M. Gorgievski, D. Božić, V. Stanković, N. Štrbac, S. Šerbula, *Ecol. Eng.* 58 (2013) 113-122
- [18] V.D. Stanković, *Fenomeni prenosa i operacije u metalurgiji-2 Prenos toplote I mase*; Univerzitet u Beogradu, Tehnički fakultet, Bor, Srbija (1998) (In Serbian)
- [19] A. Witek-Krowiak, R.G. Szafran, S. Modelski, *Desalination* 265 (2011) 126-134
- [20] M.A.K.M. Hanafiah, W.S.W. Ngah, S.H. Zolkafly, L.C. Teong, Z.A.A. Majid, *J. Environ. Sci.* 24 (2012) 261-268
- [21] V. Murphy, S. Tofail, H. Hughes, P. Mcloughlin, *Chem. Eng. J.* 148 (2009) 425-433
- [22] A. Girao, G. Caputo, M.C. Ferro, *Compr. Anal. Chem.* 75 (2017) 154-166
- [23] D. Marković-Nikolić, A. Bojić, S. Savić, S. Petrović, D. Cvetković, M. Cakić, G. Nikolić, *J. Spectrosc.* (2018) 1-16
- [24] D. Marković-Nikolić, A. Bojić, D. Bojić, M. Cakić, D. Cvetković, G. Nikolić, *Chem. Ind. Chem. Eng. Q.* 24 (2018) 319-332
- [25] S. Glišić, M. Cakić, G. Nikolić, B. Danilović, *J. Mol. Struct.* 1084 (2015) 345-351
- [26] G.O. El-Sayed, H.A. Dessouki, S.S. Ibrahim, *Chem. Sci. J.* 1 (2010) 1-11
- [27] R. Gill, Q. Nadeem, R. Nadeem, R. Nazir, S. Navaz, *J. Basic Environ. Sci.* 5 (2014) 306-317
- [28] T.K. Naiya, B. Singha, S.K. Das, *Proc. Int. Conf. Chem. Chem Process* (2011)
- [29] M. Zhang, *Chem. Eng. Technol.* 172 (2011) 361-368
- [30] K.K. Singh, U. Singh, A. Yadav, *J. Chem. Pharm. Res.* 3 (2011) 338-348
- [31] Y. Ho, G. Mckay, *Process Biochem.* 34 (1999)451-465
- [32] K.K. Singh, U. Singh, A. Yadav, *J. Chem. Pharm. Res.* 3 (2011) 338-348
- [33] O.A. Adelaja, I.A. Amoo, A.D. Aderibigbe, *Arch. Appl. Sci. Res.* 3 (2011) 50-60

- [34] S.R. Shukla, S.P. Roshan, J. Chem. Technol. Biotechnol. 80 (2005) 176-183
- [35] M. Sassi, B. Bestani, A.H. Said, N. Benderdouche, E. Guibal, Desalination 262 (2010) 243-250
- [36] V.B. Dang, H.D. Doan, Bioresource Technol. 100 (2009) 211-219
- [37] D. Diriba, A. Hussien, V. Rao, Bull. Environ. Contam. Toxicol. 93 (2014) 126-131
- [38] L. Chun, C. Hongzhang, Process Biochem. 39 (2004) 541-545
- [39] A. Gao, K. Xie, X. Song, K. Zhang, A. Hou, Ecol. Eng. 99 (2017) 343-348
- [40] N. Abdel-Ghani, G. El-Chaghaby, F. Helal, Desalin. Water Treat. 51 (2013) 3558-3575
- [41] J. Al-Abdullah, A. G. Al Lafi, T. Alnama, W. Al Masri, Y. Amin, M. N. Alkfri, Iran. J. Chem. Chem. Eng. 37 (2018) 131-144.

DRAGANA BOŽIĆ¹
MILAN GORGIEVSKI²
VELIZAR STANKOVIĆ²
MILORAD CAKIĆ³
SILVANA DIMITRIJEVIĆ¹
VESNA CONIĆ¹

¹Institut za rudarstvo i metalurgiju Bor,
Bor, Srbija

²Univerzitet u Beogradu, Tehnički
fakultet u Boru, Bor, Srbija

³Univerzitet u Nišu, Tehnološki fakultet
u Leskovcu, Leskovac, Srbija

NAUČNI RAD

BIOSORPCIJA JONA OLOVA IZ VODENIH RASTVORA PILJEVINOM BUKVE I PŠENIČNE SLAME

Ovaj rad predstavlja rezultate adsorpcije jona Pb^{2+} iz sintetičkih rastvora $Pb(NO_3)_2$, koristeći piljevinu bukve i pšeničnu slamu kao adsorbense. Fizičko-hemijska karakterizacija adsorbensa obuhvatala je specifičnu površinu, pH_{pzc}, SEM-EDS i FTIR analizu. Kinetika i izoterme adsorpcije, kao i promene pH rastvora tokom procesa, su praćene i analizirane. Rezultati su pokazali da je adsorpcija dobro objašnjena kinetičkim modelom pseudo-drugog reda za oba adsorbensa. Adsorpciju jona Pb^{2+} na piljevini i slami dobro opisuje izoterma Temkin, što potvrđuju visoke vrednosti koeficijenta regresije R^2 . Maksimalni adsorpcioni kapacitet jona olova na piljevini bukve i pšeničnoj slami bio je 9,9, odnosno 9,7 mg g⁻¹. Dobijeni rezultati su pokazali da su piljevina bukve i pšenična slama pogodni adsorbenti za adsorpciju jona olova iz razblaženih vodenih rastvora.

Ključne reči: biosorpcija Pb^{2+} , piljevina bukve, pšenična slama, adsorpcione izoterme.